An Improved Stator Flux Estimation in Steady-State Operation for Direct Torque Control of Induction Machines

Nik Rumzi Nik Idris, *Member, IEEE,* and Abdul Halim Mohamed Yatim, *Senior Member, IEEE,*

Abstract—This paper presents an improved stator flux estimation technique based on a voltage model with some form of low-pass (LP) filtering. In voltage-model-based stator flux estimation, an LP filter is normally used instead of a pure integrator to avoid integration drift problem due to dc offset, noise, or measurement error present in the back electromotive force. In steady-state condition, the LP filter estimator will degrade the performance and efficiency of the direct torque control (DTC) drive system since it introduced magnitude and phase errors, thus resulting in an incorrect voltage vector selection. The stator flux steady-state error between the LP filter and a pure integrator estimator technique is derived and its effect on the steady-state DTC drive performance is analyzed. A simple method is proposed to compensate for this error which results in a significant improvement in the steady-state drive performance. Simulation based on this technique is given and it is verified by experimental results.

Index Terms—Direct torque control, induction machines, stator flux, torque ripple.

I. INTRODUCTION

AN ACCURATE flux estimation in a high-performance induction motor drive, be it field-oriented or direct torque control (DTC), is important to ensure proper drive operation and stability. Most of the flux estimation techniques proposed are based on the voltage model, the current model, or a combination of both [1], [2]. The estimation based on the current model is normally applied at low frequency, and it requires the knowledge of the stator current and rotor mechanical speed or position. In some industrial applications, the use of an incremental encoder to get the speed or position of the rotor is undesirable since it reduces the robustness and reliability of the drive. It has been widely known that even though the current model has managed to eliminate the sensitivity to the stator resistance variation, the use of rotor parameters in the estimation has introduced the sensitivity of the estimation to the rotor parameter variations, especially at high rotor speed [1]–[3]. The voltage model, on the other hand, is normally used in a high speed range, since at low speed, some problems arise [3]–[5]. In

practical implementation, even a small dc offset present in the back electromotive force (EMF) due to noise or measurement error inherently present in the current sensor, can cause the integrator to saturate [4], [5]. To overcome this, a low-pass (LP) filter is normally used in place of a pure integrator. The voltage model estimation does not require the knowledge of rotor speed, and the only motor parameter used is the stator resistance, which can be measured quite accurately. These can be considered as an advantage of the voltage-model-based estimation over the current-model-based estimation technique and are also the reasons why the former is preferred over the latter in some industrial applications. However, the use of an LP filter in place of a pure integrator reduces the performance of the drive because of the phase and magnitude errors inherent in the LP filter as compared to the pure integrator, particularly at frequencies close to the cutoff.

Attempts have been made to improve the estimated stator flux based on an LP filter as given by [4]. The proposed method used an adaptive control system which was based on the fact that the back EMF is orthogonal to the stator flux. The compensator is adapted for this condition. However, to implement the proposed system requires large processor resources and longer execution time for a slower processor. The implementation of adaptive control will significantly increase the complexity of the control system, hence, it will outweigh the property of simple control structure inherent in DTC. In this paper, a phase and magnitude compensation for the voltage-model-based stator flux estimator with LP filter (which will be referred to as LP filter based) is proposed. Although the DTC technique is aimed at dynamic response, the drive steady-state response is equally important and cannot be neglected. For example, it will be shown in this paper that the phase error in the estimated flux introduced torque-ripple harmonics at $6\times$ the synchronous frequency. The proposed compensation method is very simple, yet it can improve the steady-state performance of a DTC drive significantly, particularly at a frequency close to or even smaller than the cutoff frequency. This compensation will reduce the torque harmonics, improve the stator flux locus, and extend the range of frequency that can be operated using the LP-filter-based estimator.

The remainder of the paper is organized as follows. Section II compares the estimated stator flux based on the voltage model using the pure integrator and the LP filter. The effect of the phase and magnitude errors on the steady-state drive performance are analyzed in Section III. The proposed compensation methods
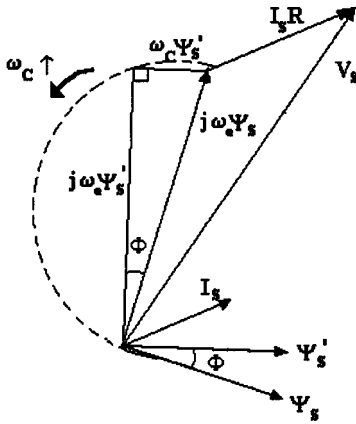
Fig. 1. Phasor diagram for steady-state operation of induction machine showing the actual and estimated stator flux based on LP filter.

are described in Section IV. Section V presents the simulation and experimental results and, finally, conclusions are given in Section VI.

II. Voltage-Model-Based Estimator

The stator flux estimation based on the voltage model is determined from the stator voltage equation given by

$$\bar{v}_s = R_s \bar{i}_s + \frac{d\bar{\psi}_s}{dt}.$$

The stator flux, therefore, can be written as

$$\bar{\Psi}_s = \int (\bar{v} - \bar{i}_s R_s)\, dt. \qquad (1)$$

Under sinusoidal steady-state condition, this reduces to

$$j\omega_e \bar{\Psi}_s = \bar{V}_s - \bar{I}_s R_s$$
$$\bar{\Psi}_s = \frac{\bar{V}_s - \bar{I}_s R}{j\omega_e}. \qquad (2)$$

To avoid the integration drift problem due to the dc offset or measurement noise, an LP filter is normally used in place of the pure integrator. With an LP filter, (2) becomes

$$\bar{\Psi}'_s = \frac{\bar{V}_s - \bar{I}_s R}{j\omega_e + \omega_c} \qquad (3)$$

where ω_c is the cutoff frequency of the LP filter in radians per second and Ψ'_s is the estimated stator flux which is obviously not equal to Ψ_s of (2). For a synchronous frequency larger than the cutoff, (2) and (3) can be graphically visualized using a phasor diagram as shown in Fig. 1.

From (2) and (3),

$$j\omega_e \bar{\Psi}_s = j\omega_e \bar{\Psi}'_s + \omega_c \bar{\Psi}'_s$$
$$\bar{\Psi}_s = \bar{\Psi}'_s - j\frac{\omega_c}{\omega_e}\bar{\Psi}'_s. \qquad (4)$$

As expected, when $\omega_e \gg \omega_c$, the LP filter estimator approaches the pure integrator estimator.

Equation (3) can be written as

$$\bar{\Psi}'_s = \frac{\bar{V}_s - \bar{I}_s R}{\omega_e^2 + \omega_c^2}(\omega_c - j\omega_e). \qquad (5)$$
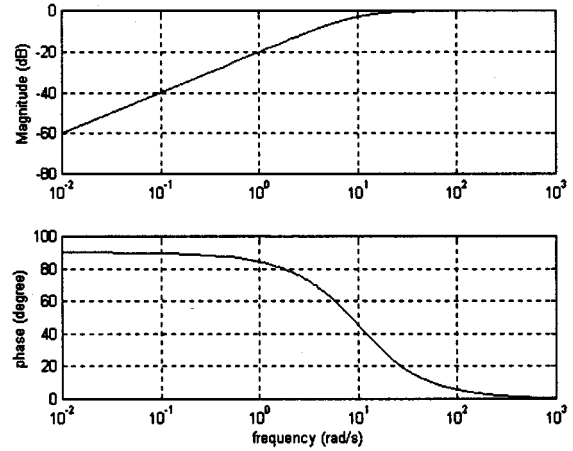

Fig. 2. Magnitude and phase frequency response of the estimated to the actual stator flux ratio.

Substituting $(\bar{V}_s - \bar{I}_s R)$ from (2) into (5),

$$\bar{\Psi}'_s = \frac{\bar{\Psi}_s}{\omega_e^2 + \omega_c^2} j\omega_e(\omega_c - j\omega_e). \qquad (6)$$

If $\bar{\Psi}'_s = \Psi'_s \angle\theta'$ and $\bar{\Psi}_s = \Psi_s \angle\theta$, then (6) can be written as

$$\frac{\Psi'_s}{\Psi_s}\angle\theta' - \theta = \frac{\omega_e}{\sqrt{\omega_e^2 + \omega_c^2}}\angle\phi \qquad (7)$$

where

$$\phi = \pi/2 - \tan^{-1}(\omega_e/\omega_c).$$

When the cutoff frequency is equal to that of the synchronous, the ratio of the estimated to the actual stator flux has a magnitude of $1/\sqrt{2}$ with an angle of $\pi/4$. It should be noted that (7) represents the ratio between the estimated and actual stator flux in sinusoidal steady-state condition. It is convenient to visualize this ratio using a plot of its magnitude in decibels and its corresponding phase difference in degree versus the synchronous speed. Fig. 2 shows such a plot with the filter cutoff frequency set to 10 rad/s. It can be seen that choosing an appropriate cutoff frequency for the LP filter estimator is very important for an optimum steady-state operation, and this depends on the operating frequency. While it is good to set the cutoff frequency as low as possible so that the phase and magnitude errors are minimized, it must be noted that this will reduce the effectiveness of the LP-filter-based estimator to filter out the dc offset which is likely present in the sensed currents or voltages. Choosing a cutoff frequency which is closer to the operating frequency will reduce the dc offset in the estimated stator flux, which on the other hand will introduce phase and magnitude errors.

III. Effect of Phase and Magnitude Errors on the DTC Drive Performance

In DTC, the selected voltage vector is based on the calculated or estimated stator flux and torque. The steady-state behavior or performance of the DTC drive is influenced by the voltage vector selections [6], [7]. As shown above, with the LP-filter-based estimator, the magnitude and phase errors exist
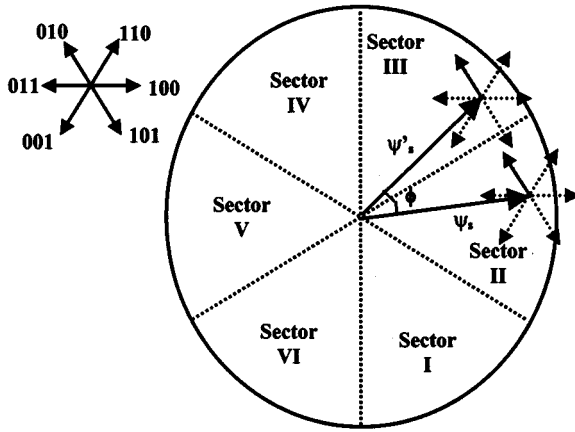
Fig. 3.   Effect of phase error on the selected voltage vectors with the actual and estimated stator flux in sectors III and II, respectively.
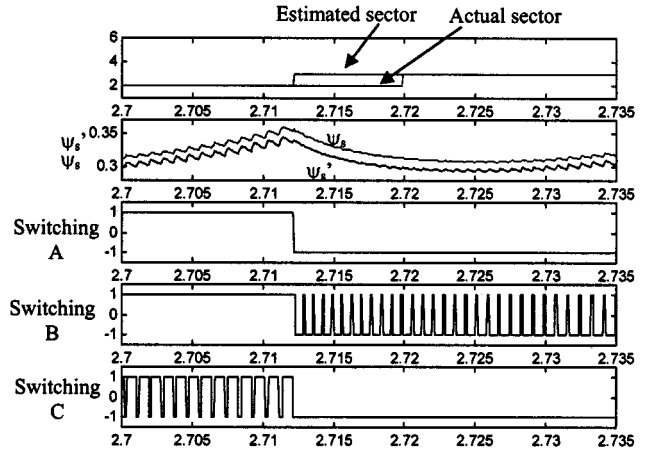

Fig. 4.   Simulation results. Traces from top—first trace: actual and estimated sector; second trace: actual and estimated stator flux; third trace: switching of phase *A*; fourth trace: switching of phase *B*; fifth trace: switching of phase *C*.

between the estimated and actual stator flux, which will definitely affect the voltage vector selections. This section will look at the effect of these errors on the stator flux locus and actual electromagnetic torque.

A. Effect on the Stator Flux

In steady state, the estimated stator flux leads the actual stator flux by an angle given in (7). The amount of phase difference depends on the cutoff frequency as well as on the synchronous frequency which will result in an incorrect voltage vectors selected in a particular sector.

The incorrect voltage vectors selected for the actual flux will give a less-than-required radial influence to the flux locus. This occurs at the end of the sector of the actual stator flux or at the beginning of the sector of LP-filter-based estimated stator flux. For example, Fig. 3 shows the estimated and actual stator flux in the stator flux plane, which are denoted by ψ_s' and ψ_s, respectively. They are assumed to rotate in the counterclockwise direction with the angle between them denoted by ϕ. Both the estimated and actual stator fluxes are in different sectors as the estimated flux enters a new sector—as shown in Fig. 3, the estimated stator flux is in sector 3 whereas the actual flux is still in sector 2. Accordingly, to increase the flux in sector 3, the controller will select voltage vector 010, however, since the actual flux is in sector 2, this voltage vector will cause a decrement rather than increment in the actual stator flux. The actual flux will only be increased with the selected voltage vector once it enters sector 3.

From Fig. 2 and (7), the magnitude of the estimated stator flux is always less than the actual stator flux. However, the difference is insignificant as $\omega_e \gg \omega_c$. Since the controller will force the estimated stator flux to follow the reference, the magnitude of the actual stator flux becomes larger than that of the reference. At high speed where the problem of flux weakening is not experienced [7], the magnitude of the actual stator flux which is larger than the rated value can result in magnetic flux saturation.

To analyze the effect of phase and magnitude errors on the selection of voltage vectors, the DTC drive is simulated using the Matlab/Simulink program. The stator flux used for the DTC

controller is estimated using an LP-filter-based estimator with the cutoff frequency set to 5 rad/s. The actual flux—which is based on pure integrator—is also calculated but is not used by the DTC controller. A closed-loop speed control is utilized with the speed reference set to 20 rad/s. The selection of voltage vectors is made as proposed in [8]. Fig. 4 shows the waveform with the time axis zoomed in the vicinity where the stator flux is moving toward sector 3 from sector 2. According to [8], to increase the torque and flux in sectors 2 and 3, voltage vectors 110 and 010 should be selected, respectively. Choosing voltage vector 010 in sector 2 will result in a decrease in stator flux. Since the selection is made based on the estimated stator flux position, the actual stator flux will decrease (when it should be increased) during the period when the estimated and actual flux stator are in different sectors. Consequently, in steady state, particularly at low speed, the magnitude of the actual flux will be reduced and its locus tends to become hexagonal in shape.

B. Effect on Electromagnetic Torque

The torque controller will ensure that the estimated torque equals the reference. If a synchronous rotating reference frame is chosen such that its d axis is aligned with the estimated stator flux, the torque expression is given by (8). The voltage vectors will be selected accordingly such that the product of the q component of the stator current and the stator flux magnitude will follow the reference torque within its hysteresis band

$$T_e' = \frac{3}{2}\frac{p}{2}\psi_s' i_{sq}^{\psi s'}. \tag{8}$$

In (8), ψ_s' is the estimated stator flux and $i_{sq}^{\psi s'}$ is the q component of the stator current in the estimated stator flux reference frame, which is shown in Fig. 5.

Since there is a phase difference between the actual and estimated stator flux, the actual torque expression will contain the product of the d component stator current and q component of the actual stator flux as given by

$$T_e = \frac{3}{2}\frac{p}{2}\left(\psi_{sd}^{\psi s'} i_{sq}^{\psi s'} - \psi_{sq}^{\psi s'} i_{sd}^{\psi s'}\right). \tag{9}$$
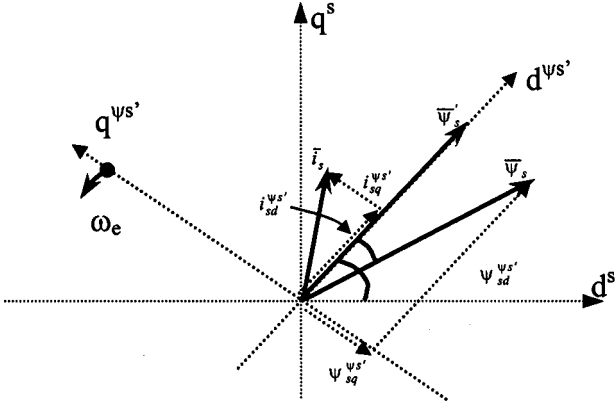
Fig. 5.   Space vectors of stator current, actual stator flux, and estimated stator flux with rotating and stationary reference frame.

In (9), $\psi_{sd}^{\psi s'}$ and $\psi_{sq}^{\psi s'}$ are the d and q components of the actual stator flux in the estimated stator flux reference frame. In steady state with constant reference torque, the second term of the right-hand side of (9) results in a harmonics ripple at $6\times$ the synchronous frequency present in the actual torque.

IV.   IMPROVED VOLTAGE-MODEL-BASED STATOR FLUX ESTIMATOR

The purpose of replacing the pure integrator with the LP filter in the stator flux estimator is to avoid the integration drift problem due to the dc offsets present in the sensed currents or voltages. It has been shown that the phase and magnitude errors of the estimated stator flux introduced by the LP filter affected the selection of voltage vectors and the electromagnetic torque response and, hence, degraded the performance of the DTC drive. The core of the proposed improvement is to provide the magnitude and phase compensations for the estimated flux, under steady-state condition, only at the operating frequency, thus improving the steady-state performance of the DTC drive. In other words, the LP filter action is effective at all frequencies except at the operating frequency, that is,

$$\psi_S' = \begin{cases} \frac{v - iR}{s}, & \text{for } \omega = \omega_e \\ \frac{v - iR}{s + \omega_c}, & \text{for } \omega \neq \omega_e. \end{cases} \tag{10}$$

The LP filter action is, therefore, valid or effective for the dc offsets and low-frequency components present in the sensed currents or voltages. This means that the integration drift problem is avoided while at the same time good system stability is maintained since the phase and magnitude errors are compensated at the operating frequency. The d and q axes of the stator flux are compensated at the operating frequency by determining the expressions for the actual stator flux in terms of estimated stator flux.

From the angle relation of (7), the d component of the actual stator flux is given by

$$\psi_{sd} = \psi_s \cos(\theta' - \phi)$$

where $\phi = \pi/2 - \tan^{-1}(\omega_c/\omega_e)$.

Let $\phi' = \tan^{-1}(\omega_e/\omega_c)$, hence,

$$\psi_{sd} = \psi_s \sin(\theta' + \phi')$$
$$\psi_{sd} = \psi_s(\sin\theta' \cos\phi' + \sin\phi' \cos\theta')$$
$$\psi_{sd} = \psi_s \left(\frac{\psi_q'}{\psi_s'} \frac{\omega_c}{\sqrt{\omega_c^2 + \omega_e^2}} + \frac{\psi_d'}{\psi_s'} \frac{\omega_e}{\sqrt{\omega_c^2 + \omega_e^2}} \right)$$
$$\psi_{sd} = \frac{\sqrt{\omega_c^2 + \omega_e^2}}{\omega_e} \psi_s' \left(\frac{\psi_q'}{\psi_s'} \frac{\omega_c}{\sqrt{\omega_c^2 + \omega_e^2}} + \frac{\psi_d'}{\psi_s'} \frac{\omega_e}{\sqrt{\omega_c^2 + \omega_e^2}} \right)$$
$$\psi_{sd} = \left(\psi_q' \frac{\omega_c}{\omega_e} + \psi_d' \right). \tag{11}$$

Similarly, for the q axis,

$$\Psi_{sq} = -\Psi_s \cos(\theta' + \phi')$$
$$\Psi_{sq} = -\Psi_s(\cos\theta' \cos\phi' - \sin\phi' \sin\theta')$$
$$\Psi_{sq} = \Psi_s \left(-\frac{\Psi_d'}{\Psi_s'} \frac{\omega_c}{\sqrt{\omega_c^2 + \omega_e^2}} + \frac{\Psi_q'}{\Psi_s'} \frac{\omega_e}{\sqrt{\omega_c^2 + \omega_e^2}} \right)$$
$$\Psi_{sq} = \frac{\sqrt{\omega_c^2 + \omega_e^2}}{\omega_e} \Psi_s' \left(-\frac{\Psi_d'}{\Psi_s'} \frac{\omega_c}{\sqrt{\omega_c^2 + \omega_e^2}} + \frac{\Psi_q'}{\Psi_s'} \frac{\omega_e}{\sqrt{\omega_c^2 + \omega_e^2}} \right)$$
$$\Psi_{sq} = \left(-\Psi_d' \frac{\omega_c}{\omega_e} + \Psi_q' \right). \tag{12}$$

Equations (11) and (12) give the relations between d and q components of the actual stator flux in terms of the d and q components of the estimated stator flux at the operating frequency. To implement the compensation, we need to know the cutoff frequency of the LP filter, ω_c and the operating frequency ω_e. The average stator flux frequency ω_e is obtained from (13) [3], [7]

$$\omega_e = -\frac{(\bar{v} - \bar{i}_s R_s)}{\Psi_s^2} \cdot j\bar{\Psi}_s. \tag{13}$$

The block diagram of the DTC drive with the compensation scheme in detail is as shown in Fig. 6(a) and (b). The input to the compensator is the d and q components of the estimated stator flux, the reciprocal of synchronous frequency, and the flag to activate the compensator. When activated, the flag will equal 1, otherwise it will equal zero. With zero flag, $\Psi_d' = \Psi_d$ and $\Psi_q' = \Psi_q$. The flag can be manually activated or it can be automatically activated based on the steady-state speed or synchronous speed. Once activated, the stator flux will be compensated—this is done by adding the d and q components of the estimated stator flux based on the LP filter with the compensation values as given by (11) and (12). It should be noted that the analysis done above is based on sinusoidal steady-state condition, hence, the compensation is only valid for steady-state conditions. Nevertheless, as will be shown in the next section, this compensation scheme has managed to improve the stator flux locus as well as almost completely eliminate the torque harmonics ripple.

V.   SIMULATION AND EXPERIMENTAL RESULTS

To verify the proposed stator flux estimator, simulations and experiments on the DTC induction motor drive were carried out.
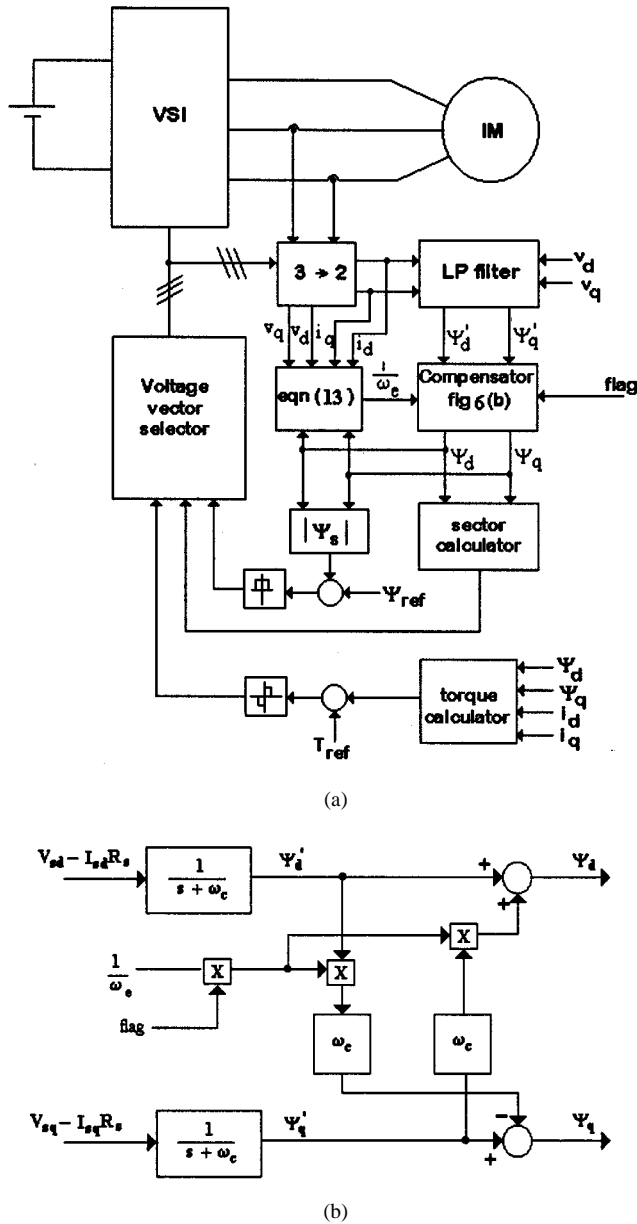
Fig. 6. Block diagram of the improved stator flux estimator. (a) DTC drive incorporating the flux compensator. (b) Stator flux compensator in detail.

The simulations were performed using the MATLAB/Simulink simulation package, while the implementation was carried out using a dSPACE DS1102 controller board centered around a TMS320C31 digital signal processor (DSP) at 60 MHz.

A. Experimental Setup

The experimental setup is shown in Fig. 7 and consists of a standard 1/4-hp induction machine, insulated-gate-bipolar-transistor (IGBT)-based three-phase inverter, the dSPACE controller card, and Xilinx field-programmable gate array (FPGA). A standard Pentium-based PC is used to host the controller board and the FPGA systems. To reduce the computation burden of the DSP, some of the main tasks are performed by the FPGA. The main tasks are summarized as follows.
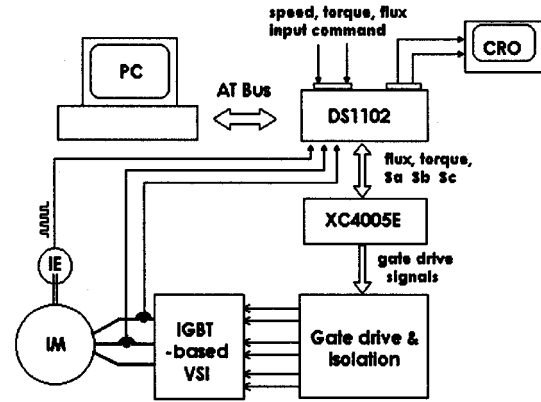

Fig. 7. Experimental setup.

dSPACE:
- torque and stator flux hysteresis comparators;
- torque and stator flux estimations based on LP filter;
- calculation of the stator flux compensation values.

Xilinx FPGA:
- voltage vector selection;
- blanking time for the VSI switches;
- protections.

With this configuration and the sharing of the tasks between the DSP and the FPGA, the sampling period is reduced to 55 μs.

B. Simulation and Experimental Results

The DTC drive for both simulation and experiment were run without the speed loop. In the experimental setup, a dc machine is used to load the drive. The dc-link voltage of the inverter is set to 120 V and the torque command is set to 0.2 N·m (30% of the rated torque). The machine is loaded to give a steady-state speed of 20 rad/s. Since the machine is run without the outer speed loop, with higher reference torque, it is difficult to have the machine avoid entering its flux-weakening mode. The compensation is applied at $t = 5$ s for the simulations and at the instant the flag signal becomes "high" for the experiments.

Fig. 8 shows the simulation results of the actual d and q axes of the stator flux, and the magnitude of the stator flux before and after the compensation is applied with the LP filter cutoff frequency set to 5 rad/s. Before the compensation, the stator flux magnitude shows some weakening due to the incorrect voltage vector selection, as discussed earlier. The phase error and magnitude deterioration can be seen from the d–q component of the stator flux which is significantly distorted before the compensation. The shape of the stator flux locus before the compensation is approaching that of the hexagonal, as shown in Fig. 9(a). After the compensation, the circular locus of the stator flux is restored with its magnitude increased [Fig. 9(b)]. Due to the hexagonal shape of the stator flux and the phase error in the estimated stator flux, the actual torque contained harmonics at $6\times$ the fundamental frequency (as discussed in Section III) and is shown in Fig. 10. Once the compensation is applied at $t = 5$ s, the ripple is eliminated because the stator flux phase angle is compensated and the circular stator flux locus is restored. The estimated torque is maintained constant by the controller.
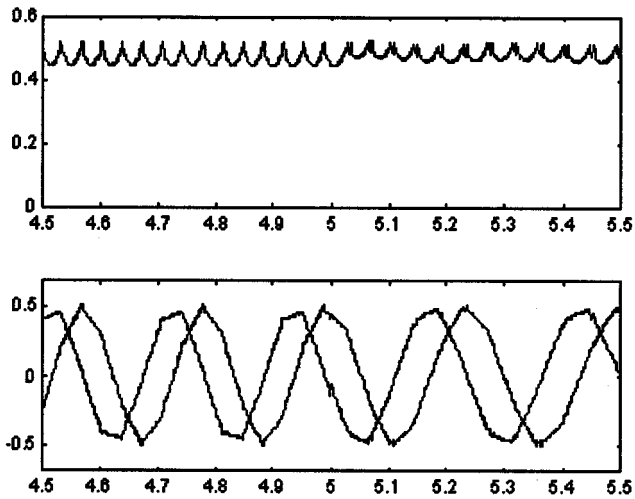
Fig. 8.   Simulation results. Top trace: actual stator flux; bottom trace: d and q axes of estimated stator flux with $\omega_c = 5$ rad/s.
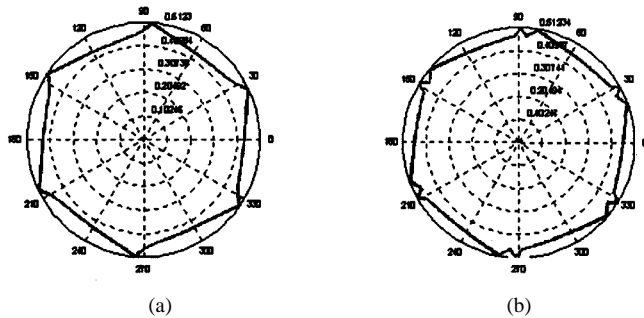

Fig. 9.   Simulation results with $\omega_c = 5$ rad/s. Stator flux locus (a) before compensation and (b) after compensation.
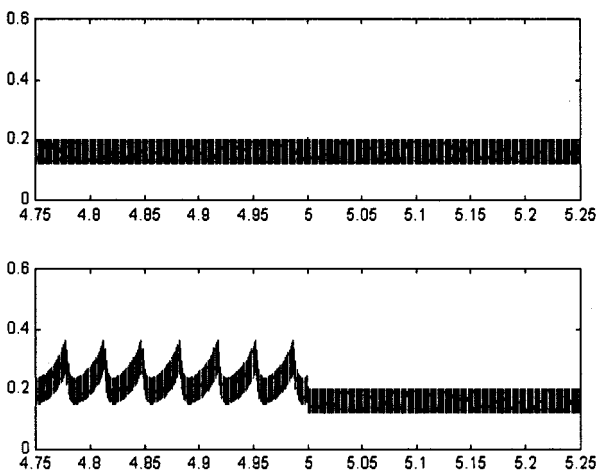

Fig. 10.   Simulation results. Top trace: estimated torque; bottom trace: actual torque. $\omega_c = 5$ rad/s.

Experiments were carried out under the same conditions as the simulation. Fig. 11 shows the d and q axes of the estimated stator flux and the magnitude of the stator flux before and after the compensation is applied, while Fig. 12(a) and (b) shows the stator flux locus before and after the compensation, respectively. Fig. 13 shows the estimated torque, which is calculated using the compensated stator flux, and the estimated torque which is used
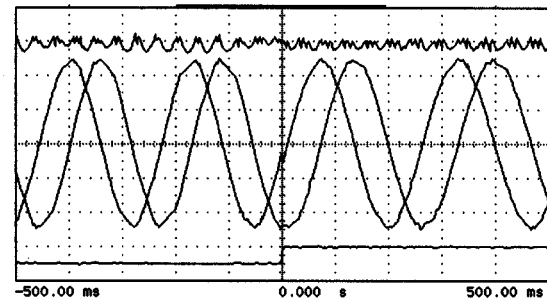

Fig. 11.   Experimental results. Top trace: stator flux magnitude (0.1 Wb/div); middle trace: estimated stator flux d and q axes (0.2 Wb/div); bottom trace: flag signal. $\omega_c = 5$ rad/s.
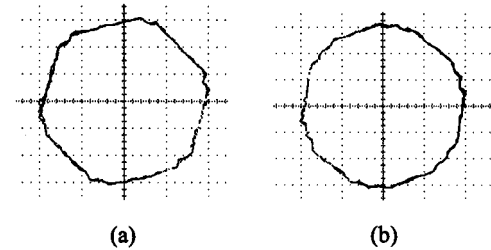

Fig. 12.   Experimental results, $\omega_c = 5$ rad/s. Stator flux locus (a) before compensation and (b) after compensation.
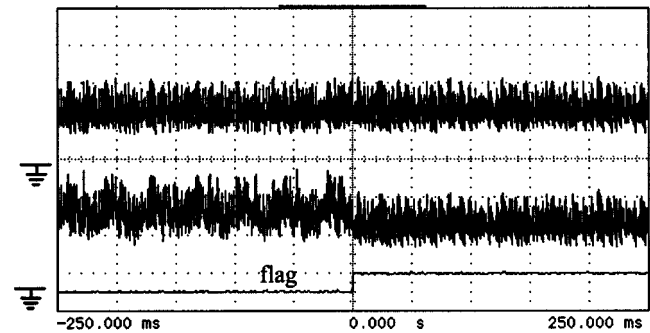

Fig. 13.   Experimental results. Top trace: estimated torque used by the controller (0.1 N·m/div); bottom trace: estimated torque calculated using the compensated stator flux (0.1 N·m/div). $\omega_c = 5$ rad/s.

by the controller. The former closely approximates the actual torque, which cannot be measured in the experiments. It can be seen that the simulation and experimental results are in close agreement.

VI. CONCLUSION

This paper has presented the effect of using an LP filter in place of a pure integrator in the voltage-model-based stator flux estimator to the steady-state performance of the DTC of an induction motor drive system. A compensation scheme to eliminate the phase and magnitude errors for the stator flux estimation under steady-state condition was proposed. The validity of the proposed compensation scheme was supported with extensive simulation and experimental results. It is shown that the simple proposed compensation scheme results in improved stator flux and torque responses of the DTC drive under steady-state condition.

APPENDIX

The motor parameters used for the simulation and experiment are as follows: 240 V, 50 Hz, 1/4 hp, two-pole, squirrel cage.

$$R_s = 10.9\,\Omega, \quad R_r = 9.25\,\Omega, \quad L_r = 0.858\,792\,\text{H}$$
$$L_s = 0.858\,792\,\text{H}, \quad L_m = 0.828\,981\,\text{H}.$$

REFERENCES

[1] P. L. Jansen and R. D. Lorenz, "A physically insightful approach to the design and accuracy assessment of flux observers for field oriented induction machine drives," *IEEE Trans. Ind. Applicat.*, vol. 30, pp. 101–110, Jan./Feb. 1994.
[2] M. Elbuluk, N. Langovsky, and M. D. Kankam, "Design and implementation of a closed-loop observer and adaptive controller for induction motor drives," *IEEE Trans. Ind. Applicat.*, vol. 34, pp. 435–443, May/June 1998.
[3] T. G. Habetler, F. Profumo, G. Griva, M. Pastorelli, and A. Bettini, "Stator resistance tuning in stator flux field-oriented drive using an instantaneous hybrid flux estimator," *IEEE Trans. Power Electron.*, vol. 13, pp. 125–133, Jan. 1998.
[4] J. Hu and B. Hu, "New integration algorithms for estimating motor flux over a wide speed range," *IEEE Trans. Power Electron.*, vol. 13, pp. 969–976, Sept. 1998.
[5] K. D. Husrt, T. G. Habetler, G. Griva, and F. Profumo, "Zero speed tacholess IM torque control: Simply a matter of stator voltage integration," *IEEE Trans. Ind. Appl.*, vol. 34, pp. 790–795, July/Aug. 1998.
[6] D. Casadei, G. Grandi, G. Serra, and A. Tani, "Effect of flux and torque hysteresis band amplitude in direct torque control of induction motor," presented at the IEEE IECON'94, Bologna, Italy, Sept. 5–9, 1994.
[7] ——, "Switching strategies in direct torque control of induction machine," presented at the International Conf. Electrical Machines, Paris, France, Sept. 5–8, 1994.
[8] I. Takahashi and T. Noguchi, "A new quick-response and high-efficiency control strategy of an induction motor," *IEEE Trans. Ind. Applicat.*, vol. IA-22, pp. 820–827, Sept./Oct. 1986.

Nik Rumzi Nik Idris (M'96) received the B.Eng. degree in electrical engineering from the University of Wollongong, Wollongong, Australia, the M.Sc. degree in power electronics from Bradford University, Bradford, U.K., and the Ph.D. degree from the Universiti Teknologi Malaysia, Skudai, Malaysia, in 1989, 1993, and 2000, respectively.

Currently, he is a Lecturer at the Universiti Teknologi Malaysia. His research interests include ac drive systems and DSP applications in power electronics systems.

Dr. Idris is a member of the IEEE Industry Applications and IEEE Power Electronics Societies.

Abdul Halim Mohamed Yatim (M'89–SM'01) received the B.Sc. degree in electrical and electronics engineering from Portsmouth Polytechnic, Portsmouth, U.K., and the M.Sc. and Ph.D. degrees in power electronics from Bradford University, Bradford, U.K., in 1981, 1984, and 1990, respectively.

Since 1982, he has been a member of the faculty at the Universiti Teknologi Malaysia, Skudai, Malaysia, where he is currently a Professor and Head of the Energy Conversion Department. He has been involved in several research projects in the areas of power electronics applications and drives. He was a Commonwealth Fellow in 1994–1995 at Heriot-Watt University, U.K., and a visiting scholar at the Virginia Power Electronics Center in 1993.

Dr. Yatim is an active member of the IEEE Malaysian Section and a corporate member of the Institution of Engineers Malaysia. He is a Registered Professional Engineer with the Malaysian Board of Engineers.